Periodic reactor operation for parameter estimation in catalytic heterogeneous kinetics. Case study for ethylene adsorption on Ni/Al2O3

Caroline Urmès, Joanne Obeid, Jean-Marc Schweitzer, Amandine Cabiac, Carine Julcour-Lebigue, Yves Schuurman

Periodic reactor operation for parameter estimation in catalytic heterogeneous kinetics. Case study for ethylene adsorption on Ni/Al_2O_3

Caroline Urmès [a,c], Joanne Obeid [a], Jean-Marc Schweitzer [c], Amandine Cabiac [c], Carine Julcour [b], Yves Schuurman [a,*]

[a] Univ Lyon, Université Claude Bernard Lyon 1, CNRS, IRCELYON - UMR 5256, 2 Avenue Albert Einstein, 69626 Villeurbanne Cedex, France
[b] Laboratoire de Génie Chimique, Université de Toulouse, CNRS, INPT, UPS, Toulouse, France
[c] IFP Energies nouvelles, Etablissement de Lyon, Rond-point de l'échangeur de Solaize, BP3, 69360 Solaize, France

GRAPHICAL ABSTRACT

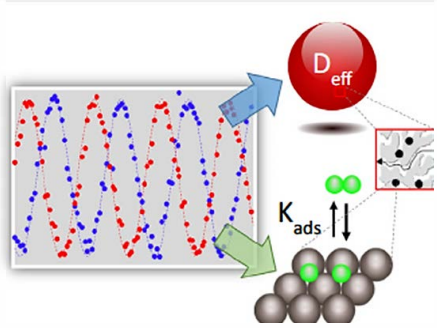

ABSTRACT

Periodic operation of chemical reactors has usually been analyzed for a potential gain in performance. However, at the laboratory scale, periodic operation of a catalytic reactor can be used for kinetic studies with better parameter estimation, which is inherent to transient kinetic studies.

Different mathematical methods are developed and compared in this study to simulate and model con centration cycling in a fixed bed catalytic reactor. Different cases including dissociative and molecular adsorption are considered with or without external and internal mass transfer limitations. The analysis of these cases gives information on the contribution of the different parameters on the phase lag and gain loss. This information can be used to better plan experimental kinetic studies.

Ethylene adsorption over a Ni/Al_2O_3 catalyst has been studied experimentally in a dedicated set up with a high speed Infrared analyzer capable of analyzing the outlet gas mixture with a data acquisition frequency up to 30 Hz. The data are modeled with one of the analytical expressions developed in this work to estimate the equilibrium adsorption constant.

1. Introduction

Periodic operation of chemical reactors has been of interest to chemical engineers in the last few decades, as it allows in certain cases to increase the reactor performance (Silveston et al., 1995). More recently, the importance of reactor/reaction dynamics has been stressed in the area of renewable resources where large fluc tuations in flow and gas composition can occur (Kalz et al., 2017). At the laboratory level, periodic operation of a catalytic reactor allows to get more detailed insight into the reaction mechanism and better parameter estimates of the underlying reactions

Nomenclature

a_s	external surface area of the catalyst, $m^2\ m^{-3}$
C	concentration, mol m^{-3}
C_{NM}	concentration of active site, mol m^{-3}
D_{eff}	effective diffusion, $m^2\ s^{-1}$
f	frequency, Hz
F	molar flowrate, mol s^{-1}
H	gain, ( )
ΔH_{ads}	adsorption enthalpy, kJ mol^{-1}
j	complex number, ( )
K	adsorption equilibrium constant, $m^3\ mol^{-1}$ or Pa^{-1}
k	adsorption (k_1) or desorption rate constant, (k_{-1}) $m^3\ mol^{-1}\ s^{-1}$ or s^{-1}
k_{gs}	gas solid mass transfer coefficient, m s^{-1}
L_R	reactor length, m
r_{Kj}	rate of an elementary step, s^{-1}
r	radial coordinate in the particle, m
r_p	particle radius, m
ΔS_{ads}	adsorption entropy, kJ $mol^{-1}\ K^{-1}$
t	time, s
T_R	residence time based on the interstitial gas and the gas in the pores, s
T_{R_2}	residence time based on the interstitial gas, s
v_{sg}	gas velocity, m s^{-1}
ω	angular frequency ($2\pi f$) radians, s^{-1}
X_{amp}	amplitude of the oscillation, %mol
z	spatial discretization, m

Subscript

p	particle
i	number of the component
j	number of the reaction
0	initial

Superscript

g	gas
in	inlet
out	outlet
s	solid
ss	steady state

Symbols

*	active site
θ	fractional surface coverage
ϕ	phase shift
Δ	perturbation term
ε	bed porosity
ε_p	particle porosity
μ_{ij}	stoichiometric coefficient

(Berger et al., 2008). Several studies have shown that concentration modulation can be used for model discrimination (Thullie and Renken, 1993; Marcelin et al., 1986; Yasuda et al., 1991). Periodic operation has been used to study processes occurring in car exhaust catalyst (Lie et al., 1993) or to estimate diffusion coeffi cients in micro/mesoporous materials (Spivey et al., 1994). On the other hand only few studies are reported where the approach is used for parameter estimation of catalytic reactions. Drawbacks of unsteady state kinetics are the more elaborate experimentation required and mostly the mathematical complexity necessary to access to the kinetics.

Several different approaches have been developed during the last few decades to analyze the dynamics under periodic reactor operation (Marković et al., 2008; Meyer et al., 2017; van Neer et al.,1996; Alvarez et al., 2012; Watanabe et al., 1981). A recent review describes the use of nonlinear frequency response methods to improve process performance (Petkovska et al., 2018). All these studies focus on developing mathematical tools to maximize the reaction rate under periodic conditions. Only a few studies have focused on the investigation of the kinetics and the determination of rate parameters. Li et al. (1989) measured the adsorption and desorption rate constants for CO over Pt/SiO_2 from modulated FTIR experiments (Fourier Transform Infrared Spectroscopy). Hoebink et al. (1999) were able to estimate nearly all parameters of a 7 steps reaction mechanism for CO oxidation over Pt/Al_2O_3 from con centration cycling experiments. Reyes et al. investigated the plat inum catalyzed dehydrogenation of methyl cyclohexane into toluene (Reyes et al., 2005). Garayhi and Keil employed frequency response techniques to assess kinetic parameters for methane combustion over palladium (Garayhi and Keil, 2001). Brzic and Pet kovska determined the most suitable conditions to estimate adsorption parameters by nonlinear frequency response method (Brzić and Petkovska, 2012). Steady state kinetics are usually car ried out in the absence of mass transfer limitations and under ideal flow regimes. This is not always possible under unsteady condi tions as the transport and mixing processes exhibit characteristic times that can affect the transient response. Several studies have addressed the effect of internal diffusion on the periodic operation (Park et al., 1998; Aida et al., 1999; Hertz, 2015; Kočí et al., 2004). Aida et al. stressed the importance of intrapellet diffusion and adsorption, showing that the location of the active metal inside the pellet has an effect on the reactor performance (Aida et al., 1999). In some cases, one might actually want to measure both the kinetic and transport parameters. Initial information through the use of simple models can then help to identify the operating conditions where both parameters can be measured accurately. This study aims at identifying kinetic parameters of a gas solid cat alytic reaction by periodic operation of a fixed bed reactor and sub sequent frequency analysis. We more specifically look at the effect of mass transfer limitations on the response sensitivity so as to define operation and methodology rules for a reliable evaluation of kinetic parameters. Three distinct mathematical approaches have been used. Numerical solutions of the underlying partial dif ferential equations are performed in both time and frequency domains and compared to analytical frequency responses derived from system linearization around the steady state for simple adsorption/desorption cases. The frequency analysis and the numerical solution can then be applied to more complex reactions. Finally, we assess the dynamic method for the measurement of an equilibrium adsorption constant from experimental periodic sig nals obtained during ethylene adsorption/desorption cycles over a supported nickel catalyst in a continuous flow reactor.

2. Experimental

All experiments were carried out in a fixed bed reactor, consist ing of a steel tube with an inner diameter of 3.73 mm. The reactor was immerged in a thermostatic water bath. No thermocouple was present in the reactor as, due to the low amplitude of the oscillations, no significant temperature variation was expected. The reactor pressure was measured by a pressure transducer at

the reactor inlet. Six mass flow controllers (MFC) were used to mix the inlet gases. Two of them were controlled by a 0 5 V signal gen erated from a computer controlled DAC card. The set point return was send to an ADC card, so that the actual flow was monitored directly by the computer. The test rig is presented on Fig. 1.

The reactor was loaded with 400 mg of a 20 wt.% Ni/Al_2O_3 cat alyst with a particle size in the range [100 200 μm]. The nickel dis persion is approximately 20%. No significant external or internal mass transfer limitation is expected with the chosen catalyst par ticle sizes.

The catalyst was reduced under a flow of 50 mL min ^{1} H_2 and 50 mL min ^{1} argon at 400 °C during 10 h. A high speed Infrared analyzer equipped with a light pipe as gas cell was used to analyze the products on line. The data acquisition rate of the infrared spec trometer was around 25 data points per second (25 Hz), depending on the selected resolution. The latter one was usually set to 8 cm^{-1} to favor high acquisition rates necessary to correctly trace the tran sient data.

Typical operation consisted of setting the two mass flow con trollers to a fixed set point to operate the reactor under a steady flow. Then both mass flow controllers were subjected to counter phase sinusoidal modulation at a desired amplitude and frequency for a fixed number of cycles, before getting back to steady flow. The counter phase operation insured a constant flowrate at the reactor inlet and limited pressure fluctuations. Periodic operation con sisted of mixing a steady argon flow of 160 mL min ^{1} with two sinusoidal modulated flows of CF_4 (tracer) and ethylene/argon mixture (95/5%mol) oscillating in counter phase with a mean flow rate of 20 mL min ^{1} each. The frequency of the sinusoidal flow was varied from 0.1 to 1.5 Hz with an amplitude of 5% (corresponding to a variation of ± 1 mL min ^{1} of the CF_4 and ethylene/argon mix ture flow). The tracer is used to take into account the hydrodynam ics of the experimental bench. It was assumed that CF_4 does not adsorb on the catalyst. Experiments were carried out at 25, 35 and 50 °C. The experimental conditions are summarized in Table 1.

Table 1
Operating conditions during the study of the adsorption of C_2H_4.

C_2H_4 mass flow	19 mL min ^{1} (added to 1 mL min ^{1} of argon contained in the bottle)
CF_4 mass flow	20 mL min ^{1}
Argon mass flow	160 mL min ^{1}
Catalyst weight	0.4016 g with particle size between 100 μm and 200 μm
Temperature	25 °C – 35 °C – 50 °C
Flow modulation frequency	Between 0.1 Hz and 1.5 Hz

3. Development of the numerical tools

In this study periodic oscillations of the molar flowrates are imposed, both experimentally and theoretically, by a sine function at the reactor inlet:

$$F_i \quad F_i^0(1 + X_{amp}\sin(2\pi ft + \phi_i)) \qquad (1)$$

Given that the modulation amplitude is small compared to the mean value, a linear system is supposed. As a consequence, the resulting outlet composition should oscillate at the same frequency as the inlet one.

The dynamic response of the system can then be only described by the gain, i.e. the ratio of the amplitudes, and the phase shift, which is the time lag between two periodic signals. These can be either defined between the inlet and outlet flows of the reactant or between the flows of the reactant (product) and an inert gas also introduced with periodic modulation. The former definition has been used to calculate the analytical expressions while the latter definition is used for the two other methods and the experimental data. Using a tracer simplifies the determination of time zero. The two methods have been compared for a few cases in this study and similar results were obtained. The difference between the two definitions is due to the overall residence time in the catalytic reac tor and the residence time of the gas into the pore of the catalyst. The gain and phase shift depend on the applied frequency. This dependence is evaluated in this study and the results presented as a function of the frequency (expressed in Hz). Three specific regimes can be defined for a periodic operation. At low frequency a quasi steady state regime is attained where the system is able to adjust to the slow perturbations and negligible change in the gain and phase shift occurs. In the transient regime the character istic response of the system is of the same order as the period of the modulation and this regime is especially suited to evaluate kinetic and transport parameters from the theoretical expressions or numerical calculations of the gain and phase shift. Increasing the frequency further brings the system into the relaxed steady state where the output oscillations will have a very low gain. This study is limited to a molecular reversible adsorption step with and

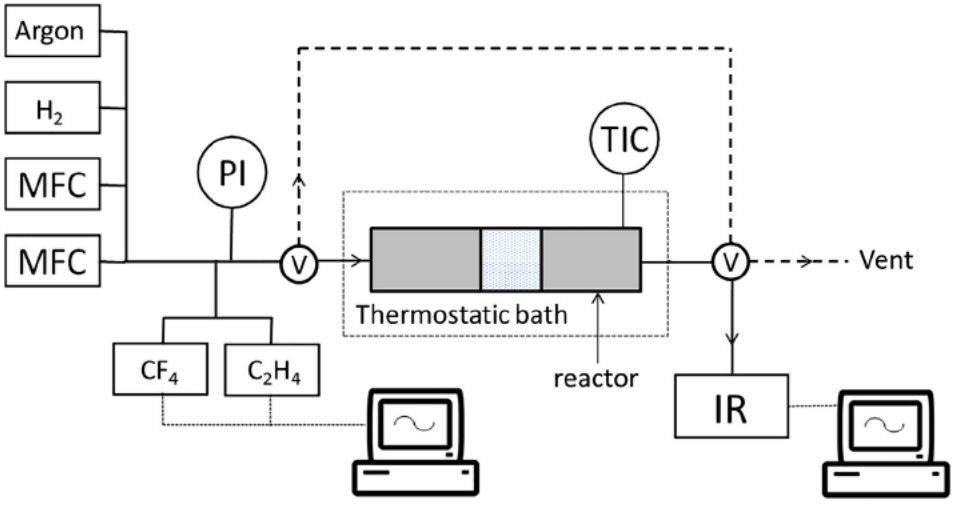

Fig. 1. Schematic of the catalyst test rig for periodic modulation of inlet gas composition in the case of CF_4 and C_2H_4 counter phase oscillations. H_2 is only used for the catalyst reduction.

without mass transfer limitations. Here the adsorption equilibrium constant is extracted from the data.

In order to keep a constant mass flow through the reactor, mass flow oscillations were performed in counter phase. Thus ϕ in Eq. (1) equals 0 for adsorbate A and π for tracer B.

3.1. Numerical solution of the model in the time domain

In order to develop the mathematical model, several further assumptions were made. The reactor has been modeled as a plug flow reactor and thus axial dispersion effects have been neglected. The reactor is assumed to be operated isothermally without any temperature gradient. Internal and external mass transfer limitations are explicitly taken into account. The change of gas velocity due to the phase shift has been neglected to better compare the numerical models with the analytical one, where the gas velocity has to be kept constant.

The reactor model consists of the partial mass balances in the gas phase, in the catalyst pores and the adsorbed phase. A mean bed porosity is considered along the axial axis.

Accounting for a uniform gas velocity, transport of component i through the reactor is modeled by:

$$\varepsilon \frac{\partial C_i^g}{\partial t} \quad v_{sg} \frac{\partial C_i^g}{\partial z} \quad k_{gs} a_S \left(C_i^g \quad C_i|_{r \ r_p} \right) \tag{2}$$

The gas solid mass transfer coefficient is estimated from the correlation of Yoshida et al. (1962) for fixed beds.

The mass balance for component i in the pores of the catalyst is given by Eq. (3).

$$\varepsilon_p \frac{\partial C_i}{\partial t} \quad \frac{D_{eff_i}}{r^2} \frac{\partial \left(r^2 \frac{\partial C_i}{\partial r} \right)}{\partial r} + C_{NM} \sum_j \mu_{ij} r_{Kj} \tag{3}$$

The binary molecular coefficient is estimated from the Fuller correlation (Poling et al., 1988). In our case, the influence of the effective diffusion on the phase lag and gain has been studied. As a consequence, fixed values of D_{eff_i} are taken for several cases. When using this equation on a real system, D_{eff_i} is obtained by accounting for the Knudsen contribution and the porous structure of the catalyst.

In the considered case, r_{Kj} refers to the adsorption and desorption rates and C_{NM} is the concentration of active adsorption sites in the catalyst. For the adsorbed phase, the mass balance is given by the following Eq. (4):

$$\frac{d\theta_i}{dt} \quad \sum_j \mu_{ij} r_{Kj} \tag{4}$$

With the limit conditions:

$$t < 0: \ C_i \quad 0, C_i^g \quad 0 \ and \ \theta^* \quad 0$$

$$t \quad 0: \ C_i^g \quad C_{i_0}^g$$

For the tracer B, the kinetic terms in Eqs. (3) and (4) are set equal to 0.

Spatial derivatives in partial differential Eqs. (2) (4) are discretized by the finite difference method, and the time integration of the resulting ordinary differential equation system is done using the LSODE solver (Radhakrishnan and Hindmarsh, 1993). The solution yields the concentration of adsorbate A and tracer B along the reactor coordinate, from which the exit flowrates are calculated. By comparing the time variations of the exit flowrates of components A and B (tracer), the corresponding gain and phase shift can be calculated. Alternatively, a discrete Fourier transform can be used to calculate the real and imaginary part of the signal, which gives the gain and phase shift directly.

A real advantage of the temporal method is that it can be applied for both linear and nonlinear cases, which does not hold for methodologies described below. As a consequence, if the amplitude tested is high, it is still possible to simulate the response of the signal by this approach.

3.2. Analytical solution of the dynamic model by Laplace transform

In case of simple reaction schemes, an analytical expression for the gain and phase shift between the inlet and outlet of a fixed bed reactor can be derived analytically, thus constituting an easy method to extract rate parameters from unsteady state experiments (Nievergeld, 1998). The amplitudes of the oscillations should be small in order to comply with linear conditions, which are required to apply the Laplace transform.

Only a molecular adsorption without mass transfer limitations will be derived here. Other cases of molecular and dissociative adsorptions including, or not, external and internal mass transfer are given in the Supporting Information.

The following reversible adsorption desorption reaction is considered:

$$A + * \underset{k \ 1}{\overset{k_1}{\rightleftarrows}} A^*$$

The mass balance for the reactant in the gas phase is given by combining Eqs. (2) (4) and neglecting concentration gradients in the film and inside the pores ($\forall r, C_i \quad C_i^g$):

$$\frac{\partial \theta_*}{\partial t} \quad k_1 C_A \theta_* \quad k \ _1 (1 \quad \theta_*) \tag{5}$$

$$(\varepsilon + (1 \quad \varepsilon)\varepsilon_p) \frac{\partial C_A}{\partial t} \quad v_{sg} \frac{\partial C_A}{\partial z} \quad C_{NM}(1 \quad \varepsilon)(k_1 C_A \theta_* \quad k \ _1 (1 \quad \theta_*)) \tag{6}$$

The inlet and outlet concentrations of A oscillate around the steady state. The concentration and the fractional surface coverage are expressed as their value at the steady state plus a perturbation term.

$$\theta_* \quad \theta_*^{ss} + \Delta\theta_*(t) \tag{7}$$

$$C_A \quad C_A^{ss} + \Delta C_A(t) \tag{8}$$

Amplitudes for the oscillations are supposed to be small to comply with linear conditions. As a consequence, terms in Δ^2 are neglected.

A Laplace transform is performed on the mass balances in adsorbed phase and in the fluid phase (external + internal). Eq. (5) gives:

$$s\Delta\theta_* \quad k_1 C_A^{ss} \Delta\theta_* + k_1 \Delta C_A \theta_*^{ss} + k \ _1 \Delta\theta_* + o(\Delta^2) \tag{9}$$

$$\text{leading to}: \ \Delta\theta_* \quad \frac{k_1 \theta_*^{ss} T_1}{sT_1 + 1} \Delta C_A \tag{10}$$

$$\text{with } T_1 \quad \frac{1}{k_1 C_A^{ss} + k \ _1} \text{ and } \theta_*^{ss} \quad \frac{k \ _1}{k_1 C_A^{ss} + k \ _1} \quad k \ _1 T_1$$

$$\text{Equation 6 gives: } (\varepsilon + (1 \quad \varepsilon)\varepsilon_p) s\Delta C_A \quad v_{sg} \frac{\partial \Delta C_A}{\partial z} \quad C_{NM}(1 \quad \varepsilon)(\quad s\Delta\theta_*) \tag{11}$$

By replacing $\Delta\theta_*$ by its expression, one obtains:

$$(\varepsilon + (1 \quad \varepsilon)\varepsilon_p) s\Delta C_A \quad v_{sg} \frac{\partial \Delta C_A}{\partial z} \quad C_{NM}(1 \quad \varepsilon) s \frac{k_1 k \ _1 T_1^2}{sT_1 + 1} \Delta C_A \tag{12}$$

An integration gives:

$$\Delta C_A^{out} \quad \Delta C_A{}^{in} e^{\left(T_R s \ T_{R2} C_{NM} \frac{k_1 k \ _1 T_1^2}{sT_1 + 1} s \right)} \tag{13}$$

with $T_R \quad (\varepsilon + (1 \quad \varepsilon)\varepsilon_p)\frac{L_R}{v_{sg}}$ and $T_{R_2} \quad (1 \quad \varepsilon)\frac{L_R}{v_{sg}}$

The transfer function of the whole reactor system in the frequency domain becomes (with $s \quad jw$):

$$H(jw) \quad e^{\left(\left(T_R \quad T_{R2}C_{NM}\frac{k_1 k_{-1}T_1^2}{1+w^2T_1^2}jw\right)\right)} e^{\left(T_{R2}C_{NM}\frac{k_1 k_{-1}T_1^3w^2}{1+w^2T_1^2}\right)} \tag{14}$$

The following expressions are then used to obtain the gain and the phase shift:

$$\left|H(w)\right| \quad \sqrt{X_R^2(w) + X_I^2(w)}$$

with X_R the real part of $H(jw)$ and X_I the imaginary part of $H(jw)$.

$$\phi \quad \arctan\left\{\frac{X_I(w)}{X_R(w)}\right\}$$

The corresponding expressions of phase shift and the gain are given in Table 2. Both the expressions for the gain and phase shift contain the individual adsorption and desorption rate constants, as well as the number of active sites. They also depend on the overall residence time in the catalytic reactor. Note that the gain and the phase shift are defined between the flow at the reactor inlet and outlet.

The expressions of the gain and the phase shift for several cases are reported below (Table 2).

The real benefit of this method is that an analytical expression allows to directly extract the parameters from the transient experiments. The method can also be applied for more complicated reactions. However, these expressions are not always easy to obtain, especially for more complicated reaction networks. Therefore another more versatile methodology will be preferred.

3.3. Frequency analysis

The numerical solution of the differential equations in the time domain is a very versatile method, but it implies to run the code for each frequency tested. In order to evaluate the response of the system as a function of the frequency, multiple runs are thus necessary, which will become very time consuming. An alternative method is to perform the estimation of the gain and the phase shift using a frequential resolution. This methodology consists of obtaining a numerical steady state solution and then of estimating the system response to an excitation in the form of an oscillation for a predefined frequency range. The mathematical development will then lead to a complex valued linear system.

Under dynamic operation, the model can be written as: $\frac{d\vec{y}}{dt} \quad \vec{f}(\vec{y}, \vec{y_E})$

with : $\vec{y} \quad \vec{y^{ss}} + \vec{x}$ and $\vec{y_E} \quad \vec{y_E^{ss}} + \vec{x_E}$

where

$\vec{y}$ is the vector of parameters to be calculated (in our case, the concentrations)
$\vec{y_E}$ is the vector of the inlet parameters
$\vec{x}$ is the resulting perturbation vector on the parameters
$\vec{x_E}$ is the vector of the perturbations performed on the inlet parameters
$\vec{y^{ss}}$ and $\vec{y_E^{ss}}$ are the vectors of steady state values of the parameters

After steady state values have been calculated, the only parameters to be solved are the components of $\vec{x}$.

The following linearization of the system can be performed:

$$\frac{d(y_1^{ss}+x_1)}{dt} \quad f_1\left(y_1^{ss}, y_2^{ss}, \ldots, y_n^{ss}, y_{E_1}^{ss}, y_{E_2}^{ss}, \ldots, y_{E_k}^{ss}\right) + \frac{\partial f_1}{\partial y_1}x_1 + \frac{\partial f_1}{\partial y_2}x_2 + \ldots + \frac{\partial f_1}{\partial y_n}x_n + \frac{\partial f_1}{\partial y_{E_1}}x_{E_1} + \frac{\partial f_1}{\partial y_{E_2}}x_{E_2} + \ldots + \frac{\partial f_1}{\partial y_{E_k}}x_{E_k}$$

$$\vdots$$

$$\frac{d(y_n^{ss}+x_n)}{dt} \quad f_n\left(y_1^{ss}, y_2^{ss}, \ldots, y_n^{ss}, y_{E_1}^{ss}, y_{E_2}^{ss}, \ldots, y_{E_k}^{ss}\right) + \frac{\partial f_n}{\partial y_1}x_1 + \frac{\partial f_n}{\partial y_2}x_2 + \ldots + \frac{\partial f_n}{\partial y_n}x_n + \frac{\partial f_n}{\partial y_{E_1}}x_{E_1} + \frac{\partial f_n}{\partial y_{E_2}}x_{E_2} + \ldots + \frac{\partial f_n}{\partial y_{E_k}}x_{E_k}$$

It can be thus written using a matrix formalism:

$$\begin{pmatrix}\dot{x_1}\\ \vdots \\ \dot{x_n}\end{pmatrix} \quad J\begin{pmatrix}x_1\\ \vdots \\ x_n\end{pmatrix} + B\begin{pmatrix}x_{E_1}\\ \vdots \\ x_{E_k}\end{pmatrix} \quad \text{or} \quad \dot{X} \quad J.X + B.X_E$$

where J and B are the following Jacobian matrixes:

Table 2
Analytical expressions for the gain and phase shift for several cases.

Molecular adsorption without mass transfer limitations

$\phi \quad w\left(-T_R - T_{R_2}\frac{C_{NM}k_1 k_{-1}T_1^2}{1+w^2T_1^2}\right)$ And $|H(w)| \quad e^{\left(T_{R_2}\frac{C_{NM}k_1 k_{-1}T_1^3w^2}{1+w^2T_1^2}\right)}$

With $T_R \quad (\varepsilon + (1-\varepsilon)\varepsilon_p)\frac{L_R}{v_{sg}}$ and $T_{R_2} \quad (1-\varepsilon)\frac{L_R}{v_{sg}}$ and $T_1 \quad \frac{1}{k_1 C_A^{ss} + k_{-1}}$

Molecular adsorption with external and internal mass transfer limitations

$\phi \quad -t_R w - \frac{3k_{gs}}{r_p}(1-\varepsilon)t_{R_2}\beta$ and $|H(w)| \quad e^{\left(\frac{3k_{gs}}{r_p}(1 \quad \varepsilon)t_{R_2}\alpha\right)}$

With α and β explained in the Supplementary Information, part 1.

$t_R \quad \varepsilon\frac{L_R}{v_{sg}}$ and $t_{R_2} \quad \frac{L_R}{v_{sg}}$

Dissociative adsorption without mass transfer limitations

$\phi \quad -w\left(T_R + \frac{4T_{R_2}C_{NM}k_1 k_{-1}(\theta^{*ss})^2\sqrt{KC_{A_2}^{ss}}}{16k_{-1}^2 KC_{A_2}^{ss} + w^2}\right)$ $\quad |H(w)| \quad e^{\left(T_{R_2}w^2\frac{k_1 C_{NM}(\theta^{*ss})^2}{16k_{-1}^2 KC_{A_2}^{ss}+w^2}\right)}$

with $\theta^{*ss} \quad \frac{1}{1+\sqrt{KC_{A_2}^{ss}}}$; $K \quad \frac{k_1}{k_{-1}}$; $T_R \quad (\varepsilon + (1-\varepsilon)\varepsilon_p)\frac{L_R}{v_{sg}}$ and $T_{R_2} \quad (1-\varepsilon)\frac{L_R}{v_{sg}}$ (see Supplementary Information part 2)

Dissociative adsorption with external and internal mass transfer limitations

$\phi \quad -t_R w - \frac{3k_{gs}}{r_p}(1-\varepsilon)t_{R_2}\beta$ and $|H(w)| \quad e^{\left(\frac{3k_{gs}}{r_p}(1 \quad \varepsilon)t_{R_2}\alpha\right)}$

With α and β explained in the Supplementary Information, part 3.

$t_R \quad \varepsilon\frac{L_R}{v_{sg}}$ and $t_{R_2} \quad \frac{L_R}{v_{sg}}$

$$J \quad \begin{pmatrix} \frac{\partial f_1}{\partial y_1} & \cdots & \frac{\partial f_1}{\partial y_n} \\ \vdots & \ddots & \vdots \\ \frac{\partial f_n}{\partial y_1} & \cdots & \frac{\partial f_n}{\partial y_n} \end{pmatrix} \quad \text{and} \quad B \quad \begin{pmatrix} \frac{\partial f_1}{\partial y_{E_1}} & \cdots & \frac{\partial f_1}{\partial y_{E_k}} \\ \vdots & \ddots & \vdots \\ \frac{\partial f_n}{\partial y_{E_1}} & \cdots & \frac{\partial f_n}{\partial y_{E_k}} \end{pmatrix}$$

The system needs to be solved in the complex domain. The out let perturbation is an oscillation written as $X \quad X_0 e^{i\omega t}$.

Inversion of the matrix system: with $\dot{X} \quad iw\ X$ leads to $X \quad (iw\ I \quad J)^{\ 1}\ B\ X_E$ (where I is the identity matrix).

The transfer function of x_i subjected to a perturbation x_{E_j} is defined as: $H_{ij}(w) \quad \frac{x_i}{x_{E_j}}$.

This transfer function gives the corresponding perturbation vec tor of the outlet parameters.

Setting $H_{ij}(w) \quad a_i + i\ b_i$, the gain and the phase shift can be obtained from the following expressions:

$$|H_{ij}(w)| \quad \sqrt{a_i^2 + b_i^2}$$

$$\tan(\phi) \quad \frac{b_i}{a_i}$$

The Jacobian matrixes have an important size because they account for the effects of the perturbation(s) on all the compo nents. However, most of the terms of these matrixes are zero. Solving such a system will be computer time demanding. As a con sequence, the SuperLU routine (http://crd legacy.lbl.gov/~xiaoye/SuperLU/, Retrieved July 3rd, 2018) has been used because it is optimized to handle sparse linear systems.

The advantage of the frequency analysis method is that the system response can be obtained easily over a full range of frequencies: calculation of the Jacobian matrixes which is time consuming has only to be performed once. However, this method can only be used for a linear case, so when the amplitudes of the oscillations are small.

4. Evaluation of the different methodologies

This section compares the three methods for solving the dynamic model as a function of the modulated flow frequency as described above in Section 3. The case of reversible molecular adsorption of a component A without mass transfer limitations is considered first (Section 4.1), while the impact of external and internal mass transport is examined in Section 4.2.

4.1. Reversible molecular adsorption

The effect of the modulated flow frequency on the gain and the phase shift is evaluated for the reversible molecular adsorption of a component A free from any mass transfer limitations. The param eters used in this study are shown in Table 3. The values are in line with the experimental case treated below. The case is simulated by

Table 3
Parameters used for the simulation.

Parameter	Value
ε	0.60
ε_p	0.56
k_1	24.84 (m^3 $mol^{\ 1}$ $s^{\ 1}$)
$k_{\ 1}$	10 ($s^{\ 1}$)
v_{sg}	0.46 (m $s^{\ 1}$)
C_{NM}	1090 (mol $m^{\ 3}$)
C_A^{ss}	4.6 (mol $m^{\ 3}$)
L_R	0.0375 (m)
r_p	75 $10^{\ 6}$ (m)

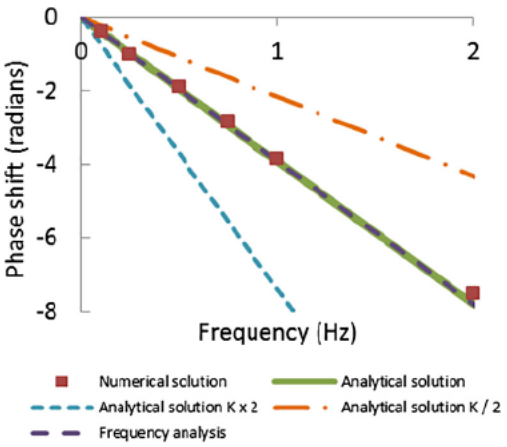

Fig. 2. Evolution of the phase shift as a function of the frequency for reversible molecular adsorption with input data of Table 3: comparison of the results given by the three methods.

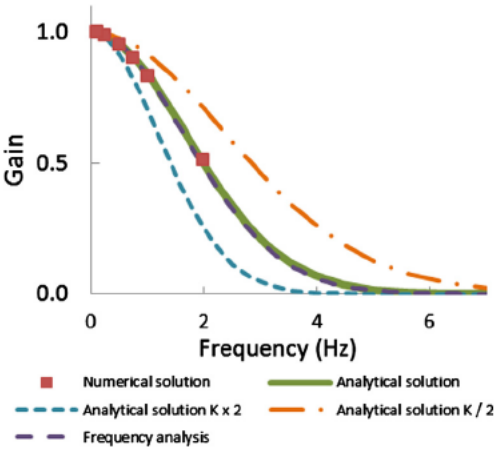

Fig. 3. Evolution of the gain as a function of the frequency for reversible molecular adsorption with input data of Table 3: comparison of the results given by the three methods.

using the analytical expression from Table 2 in Section 3.2, as well as by solving numerically the differential equations in the time domain and in the frequency domain.

The plots of the evolution of the gain and the phase shift as a function of the frequency are shown in Figs. 2 and 3. They referred to the transfer function of the system, thus the ratio of the outlet to the inlet concentrations for the adsorbate A.

As expected, the three methods give essentially the same results. A linear decrease of the phase shift with increasing fre quency is observed in Fig. 2. The slope depends on the experimen tal conditions, the concentration of active sites (C_{NM}) and the adsorption/desorption rate constants, ($k_1$and$k_{\ 1}$). Fig. 2 shows the influence of the value of the adsorption equilibrium constant ($K \quad k_1/k_{\ 1}$) on the phase shift. Actually, only the ratio of the adsorption rate constant on the desorption one is a sensitive parameter while the individual rate constants are very difficult to extract separately (see Figs. S1 and S2).

Fig. 3 shows that the experiments should be carried out below a frequency of 3 Hz; otherwise the gain will be too low, making cor rect data analysis impossible, even more if the data are noisy. On the other hand, a significant phase shift (π rad, i.e. the reactant and the tracer are completely in phase) is already obtained at ~0.8 Hz, corresponding to a time lag of 0.625 s. At that frequency, the loss in gain is less than 10%.

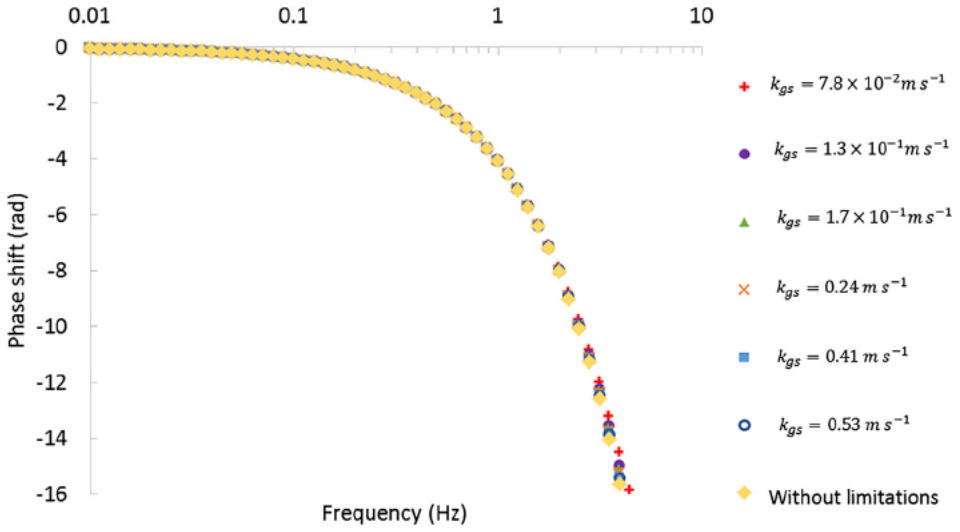

Fig. 4. Evolution of the phase shift as a function of the frequency for different values of the gas-solid mass transfer coefficient and an effective diffusivity equal to 10^{-5} $m^2\,s^{-1}$. Residence time in the reactor and particle radius are constant. Dots correspond to the analytical solution method.

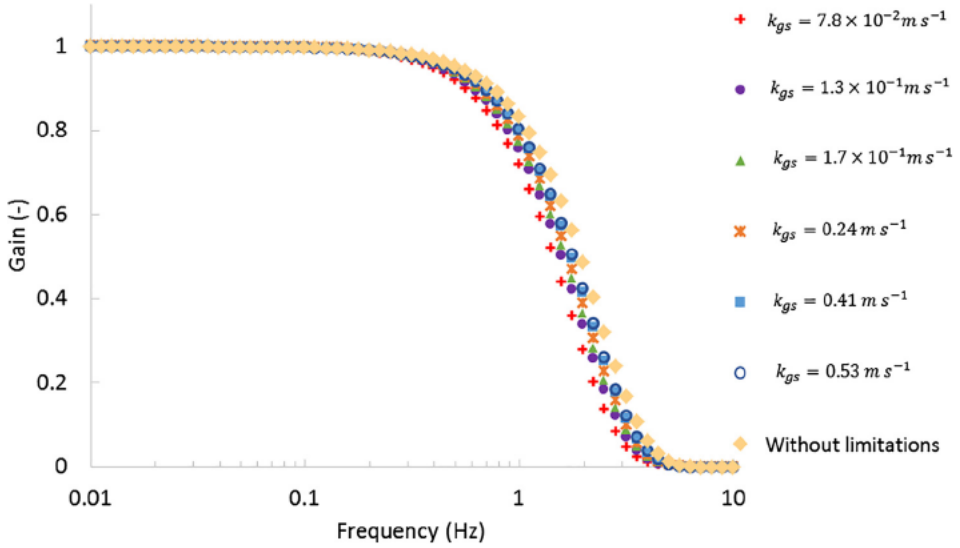

Fig. 5. Evolution of the gain as a function of the frequency for different values of the gas-solid mass transfer coefficient and an effective diffusivity equal to 10^{-5} $m^2\,s^{-1}$. Residence time in the reactor and particle radius are constant. Dots correspond to the analytical solution method.

4.2. Impact of mass transfer limitations

Next we examine the effect of external and internal mass transfer limitations during the reversible molecular adsorption with the data given in Table 3. These cases have been simulated by the analytical and the frequency analysis methods.

First, the influence of the gas solid mass transfer coefficient (k_{gs}) on the gain and the phase shift was investigated. For that purpose, the value of the effective diffusion coefficient was set to 10^{-5} $m^2\,s^{-1}$ resulting in negligible effect on the response and the particle radius was fixed to 1.5×10^{-4} m. Changes of k_{gs} were obtained by varying the gas velocity. The correlation of Yoshida et al. (1962) was used for the estimation of the gas/solid coefficient. The length of the reactor had thus to be adjusted in order to maintain a constant residence time in the reactor between the simulations ($t_R \quad \varepsilon \frac{L_R}{v_{sg}} \quad 0.05$ s). Figs. 4 and 5 show the results for the phase shift and the gain, respectively.

The results show that the increase of k_{gs} has a very small impact on the phase shift up to 3 Hz, all the curves being nearly superimposed. However, a clearer effect is observed on the gain. A drop of the gain is observed at lower frequencies with decreasing values of k_{gs}. For instance, at the value of 1 Hz, the gain varies by up to 20% on the examined k_{gs} range. If the gas solid transfer coefficient was not taken into account in this case, the equilibrium constant would be overestimated at 3.77 mol m^{-3} instead of 2.48 mol m^{-3}. As a consequence, the absence of external mass transfer limitations still has to be verified.

Next, the effect of internal diffusion limitations was examined. The external gas solid mass transfer coefficient was fixed at a value of 1 m s^{-1} in order to neglect its influence. The value of the effective diffusion coefficient was increased, while keeping all the other parameters constant. The results are shown in Figs. 6 and 7. The loss in gain occurs at lower frequencies when increasing values of the diffusion coefficient from 10^{-10} to 10^{-7} $m^2\,s^{-1}$. Thereafter the drop in gain is observed at higher frequencies until the curves overlap with that of the sorption case without any mass transfer limitations. At the lowest values of D_{eff_A} (<10^{-8} $m^2\,s^{-1}$) the phase shift curves are almost superimposed. Then the phase shift

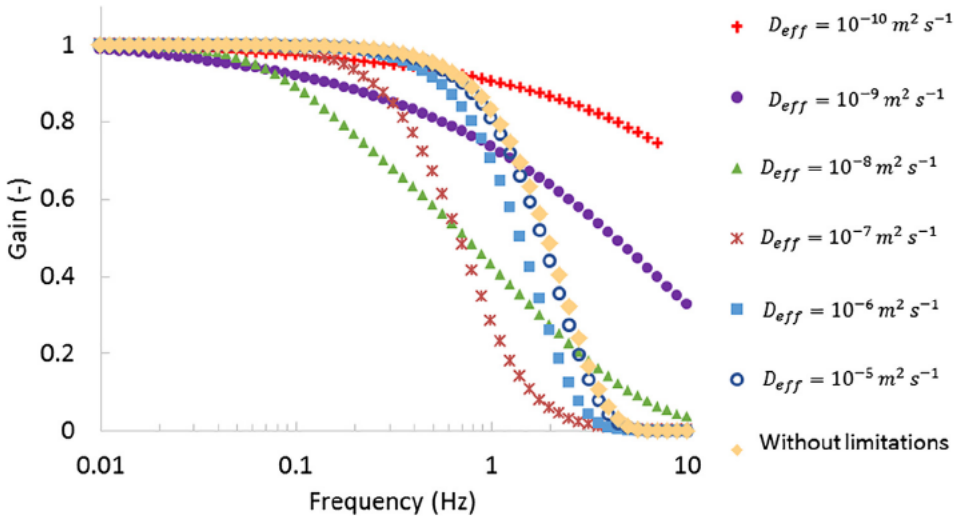

Fig. 6. Evolution of the gain as a function of the frequency for different values of the effective diffusion. The gas-solid mass transfer coefficient is equal to 1 m s ^{1}. Dots correspond to the analytical solution.

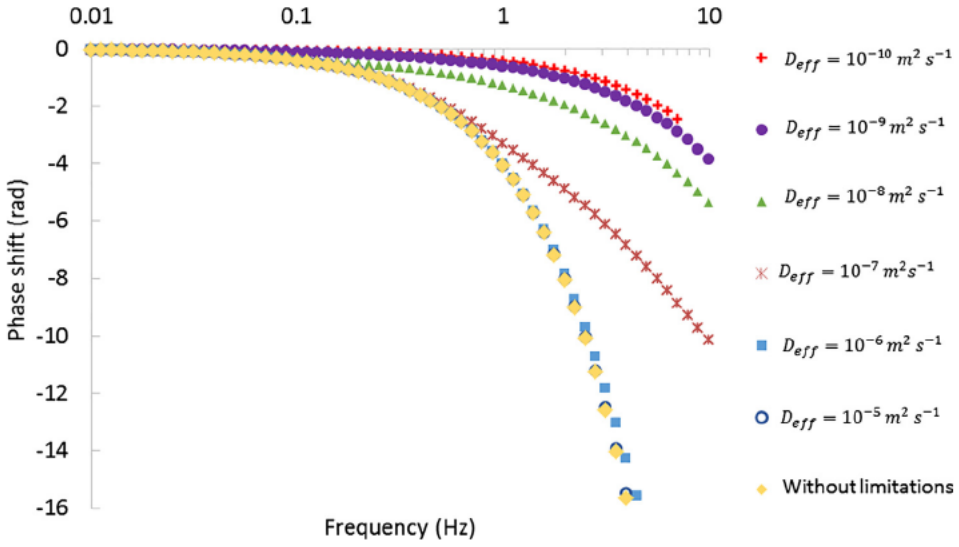

Fig. 7. Evolution of the phase shift as a function of the frequency for different values of the effective diffusion. The gas-solid mass transfer coefficient is equal to 1 m s ^{1}. Dots correspond to the analytical solution.

increases with D_{eff_A} value, until it coincides with the mass transfer resistance free case.

These trends can be explained as follows: when the character istic time of internal diffusion becomes high with respect to the period of the oscillations, the adsorbate doesn't have time to pen etrate inside the pellet during the cycle period. Thus the gain is close to 1 and the phase shift matches that observed for a simple plug flow reactor in the absence of chemical reaction (i.e $\Phi \quad t_R w$). No information about the kinetics can be thus obtained in this regime. Given the particle radius is 75 μm (cf. Table 3), the diffusion time and the period of one oscillation are in the same order of magnitude for D_{eff_A} equal to 10 ^{8} m^2 s ^{1}. The time of diffu sion is then 0.56 s and the period for a 2 Hz frequency is 0.5 s. This shows that the diffusion coefficient has to be greater than 10 ^{8} m^2 s ^{1}. If not, the diffusion time will be greater than the period.

On the other hand, in the intermediate regime which spans a large range of diffusion coefficient values, both D_{eff_A} and adsorption parameter can be estimated from the gain vs frequency curves. This is shown in Fig. 8 where a sensitivity analysis on both these parameters is performed. The value of the adsorption equilibrium constant shifts the curves with respect to the frequency, while the value of the diffusion coefficient changes the slope of the curve. By performing experiments at least for two frequencies, D_{eff_A} and K can be thus determined with good accuracy, provided a suitable frequency range has been chosen.

Another way to evaluate the impact of the effective diffusion on the gain and on the phase lag is to vary the value of the particle radius. This has been done in the Supplementary Information (part 5). In this case, the effective diffusion is constant and the radius particle varies from 5 mm to 1 μm. The values of effective diffusion coefficients taken in Fig. 8 have been used as they are in the transition range between the diffusion and the kinetic regime.

5. Experimental results

For each ethylene adsorption experiment over Ni/Al_2O_3, the by pass on the experimental set up has been used to check that CF_4

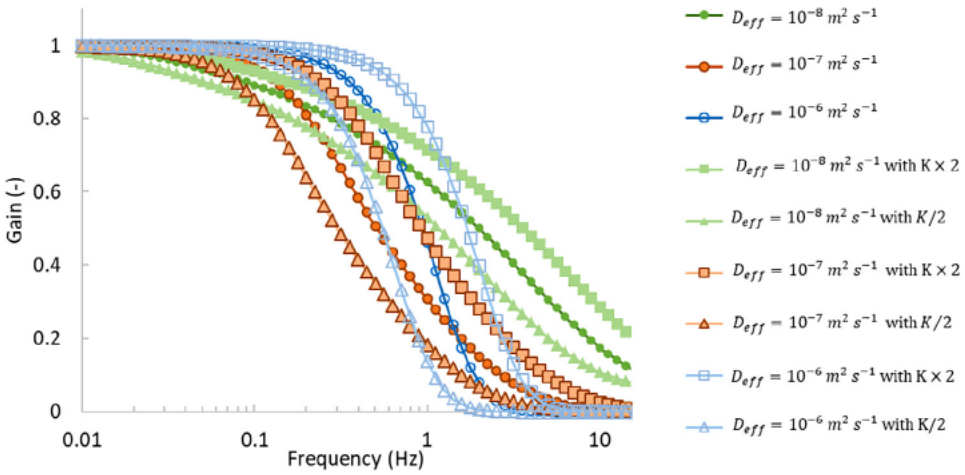

Fig. 8. Evolution of the gain as a function of the frequency for different values of effective diffusion and equilibrium adsorption constant K. The gas-solid transfer coefficient is equal to 1 m s ^{1}. The analytical solution is used for the simulations.

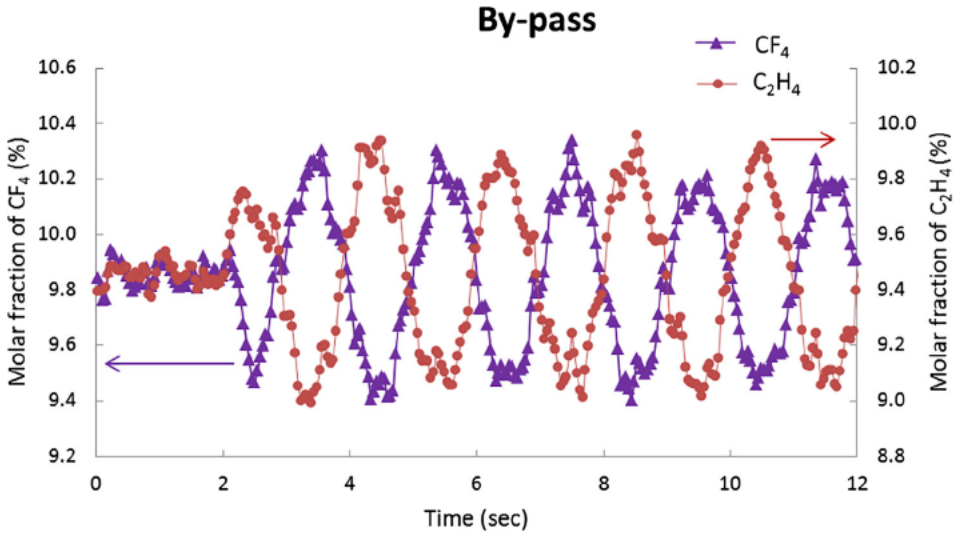

Fig. 9. Time-evolution of the molar fraction of CF_4 and C_2H_4 at the exit of the by-pass, for a frequency of 0.5 Hz and at ambient temperature. At first the catalyst is operated at steady-state conditions, then the oscillations are started (here at t ~ 2 s).

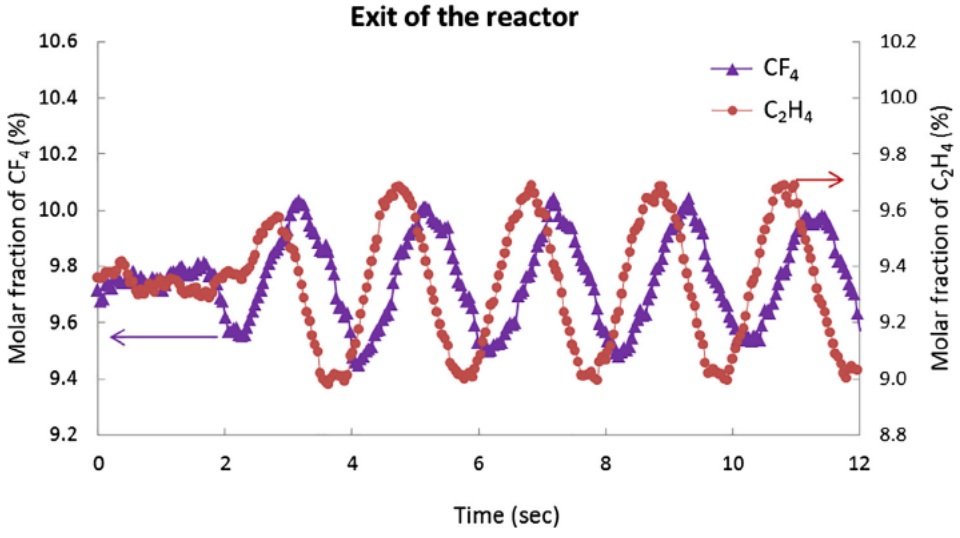

Fig. 10. Time-evolution of the molar fraction of CF_4 and C_2H_4 at the exit of the reactor, for a frequency of 0.5 Hz and at 25 °C. At first the catalyst is operated at steady-state conditions, then the oscillations are started (here at t ~ 2 s).

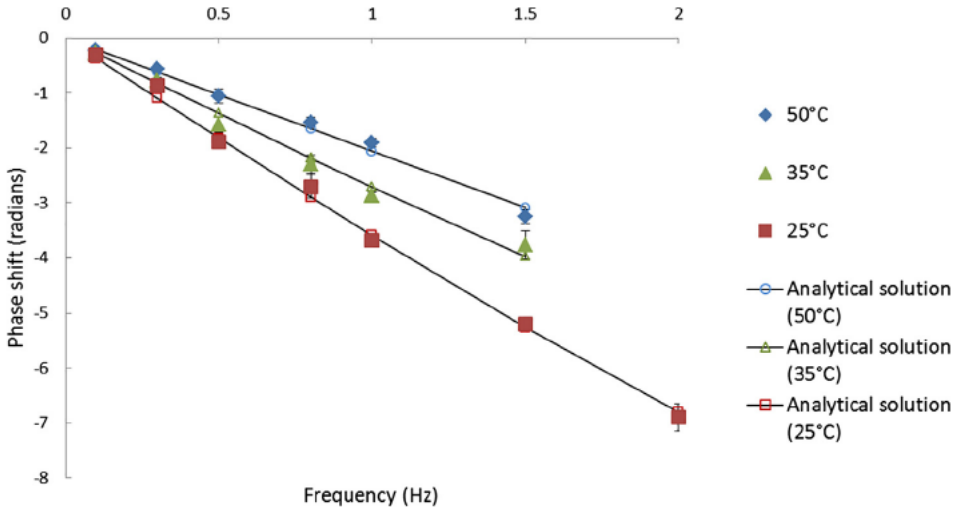

Fig. 11. Evolution of the phase shift between CF_4 and C_2H_4 as a function of the frequency for the three temperatures studied.

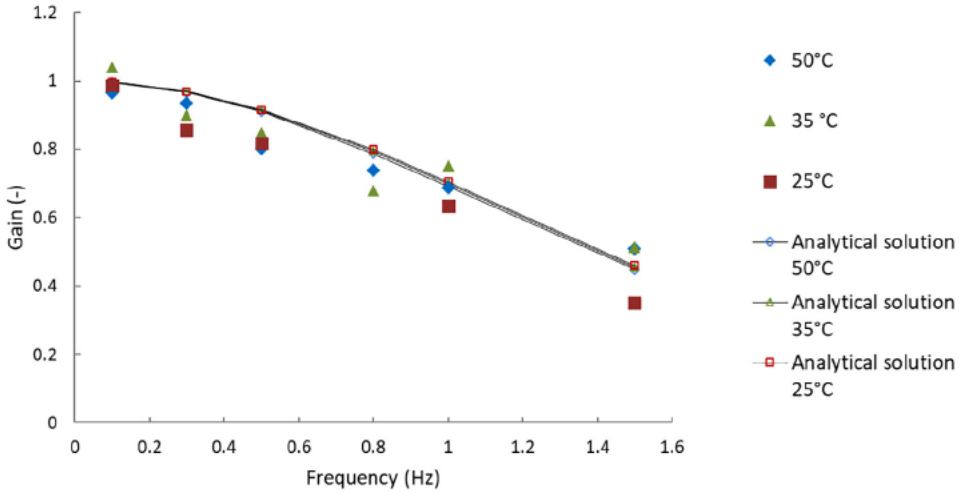

Fig. 12. Evolution of the gain for C_2H_4 as a function of the frequency for the three temperatures studied.

and C_2H_4 were correctly in counter phase. Each test was performed three times to check for the repeatability of the experiments. Figs. 9 and 10 illustrate the composition variations in CF_4 and C_2H_4 mea sured in the by pass (representative of the reactor inlet) and at the reactor outlet at a frequency of 0.5 Hz.

The plot of the experimental phase shift versus the frequency is shown in Fig. 11, together with the fit from the analytical expres sion (Table 2). The expression for molecular adsorption free from mass transfer limitations was used to fit the data. Ethylene at high concentrations adsorbs as a π bonded species, thus in a molecular state (Brown et al., 1999). The small catalyst grain size used for the experiments rules out any diffusion limitations. A linear decrease of the phase shift with increasing frequency was observed, which is well fitted by the analytical expression corresponding to the mass transfer resistance free case.

As explained before, the phase lag is obtained by subtracting the phase of the reactive, C_2H_4, and the phase of the tracer, CF_4. At the inlet of the reactor, the two components have been introduced in counter phase with a π phase shift. As a consequence, the phase shift is obtained as in Eq. (15).

$$\Phi \quad \Phi_{C_2H_4} \quad \Phi_{CF_4} \quad \pi \qquad (15)$$

From the gain as a function of the frequency, shown in Fig. 12, less information was obtained as the experimental loss in gain with increasing frequency was very similar at the three tempera tures. The loss of the gain with increasing frequency was confirmed by the simulations using the analytical expression.

The following values of the equilibrium adsorption constants were estimated (Table 4).

From the values of the equilibrium adsorption constant at the three temperatures, the adsorption enthalpy was calculated by using the Van 't Hoff equation. A linear regression fitted well ($R^2 = 0.997$) the values of ln(K) as a function of 1/T, giving a pre exponential factor of 4 10 ^{10} Pa ^{1} and an adsorption enthalpy:

Table 4
Adsorption equilibrium constants obtained.

Temperature	K (Pa ^{1})
25 °C	2.6 · 10 ^{6}
35 °C	2.0 · 10 ^{6}
50 °C	1.4 · 10 ^{6}

ΔH_{ads} 21.1 ± 5 kJ mol $^{-1}$

This corresponds to the following value of the adsorption entropy:

ΔS_{ads} 84 J mol $^{-1}$ K $^{-1}$ (reference pressure of 1 atm.)

This value fulfills the constraints given by Boudart et al. (Boudart et al., 1967) for a molecular adsorption process:

$42 < \Delta S_{ads} < S_{gas}$ 219 J mol $^{-1}$ K $^{-1}$

The limits of the inequality correspond to the loss of entropy which occurs when a gas condenses to a liquid and to the fact that a molecule cannot lose more entropy than it possesses.

The value of the enthalpy of adsorption of ethylene corresponds well to the value of 23 kJ mol $^{-1}$ measured by Iijima (1940) at low temperatures, but is much lower than the value of 120 kJ mol $^{-1}$ at 300 K at low coverages over Ni(1 0 0) obtained by Brown et al. (1999). Brown et al. observed the formation of surface species such as CCH , CH_2 and CH during ethylene adsorption. This indicates a (partly) irreversible adsorption process, while Iijima (1940) referred to a reversible van der Waals adsorption. To further inves tigate the reversibility of the adsorption of ethylene, step response experiments over Ni/Al_2O_3 were carried out. These experiments were performed after a reduction of the catalyst at 400 °C during 10 h, by switching a 4 way valve from a flow of pure argon to a mixture of Ar, CF_4 and ethylene (with a ratio as given in Table 1 and at the same temperatures as the periodic oscillation experi ments) and then switching back to pure argon. Similar amounts of adsorbed ethylene were estimated from the forward and backward switch, confirming that ethylene adsorption under these conditions is reversible (see Figs. S9 and S10). A value for the heat of adsorption of 19.5 and 24.1 kJ mol $^{-1}$ was calculated, for the forward and backward switch, respectively. Step response and periodic flow experiments thus both show a van der Waals type reversible adsorption of ethylene corresponding to a π bonded state.

6. Conclusions

We have evaluated three different mathematical methods for assessing kinetic parameters for sorption experiments over a heterogeneous catalyst by periodic flow modulation. Analytical expressions for the phase shift and gain have been derived for some simple cases for both molecular and dissociative adsorption in the absence and presence of diffusion limitations. The frequency analysis presented here is a new approach that allows to calculate quickly the gain and phase shift as a function of the frequency once a steady state solution has been calculated. Simulations using these methods have shown that in principal it should be possible to estimate both the equilibrium adsorption constant and the internal diffusion coefficient from a set of periodic modulation data as a function of the frequency. On the other hand the simulations have shown that the value of the external mass transfer coefficient has little effect on the phase shift or gain, it does have an effect on the value of the inferred equilibrium constant. Periodic flow mod ulation experiments for the sorption of ethylene over Ni/Al_2O_3, revealed a van der Waals type ethylene adsorption with an enthalpy of adsorption of 21 kJ mol^{-1}.

Appendix A. Supplementary material

Supplementary data to this article can be found online at https://doi.org/10.1016/j.ces.2018.10.012.

References

Aida, T., Na-Ranong, D., Kobayashi, R., Niiyama, H., 1999. Effect of diffusion and adsorption-desorption on periodic operation performance of NO-CO reaction over supported noble metal catalysts. Chem. Eng. Sci. 54, 4449–4457.

Alvarez, J., Meraz, M., Valdes-Parada, F., Alvarez-Ramirez, J., 2012. First-harmonic balance analysis for fast evaluation of periodic operation of chemical processes. Chem. Eng. Sci. 74, 256–265.

Berger, R., Kapteijn, F., Moulijn, J., Marin, G., De Wilde, J., Olea, M., Chen, De, Holmen, A., Lietti, L., Tronconi, E., Schuurman, Y., 2008. Dynamic methods for catalytic kinetics. Appl. Catal. A: Gen. 342 (1–2), 3–28.

Boudart, M., Mears, D.E., Vannice, M.A., 1967. Kinetics of heterogeneous catalytic reaction. Ind. Chim. Belge 32, 281–284.

Brown, W., Kose, R., King, D., 1999. The role of adsorption heats and bond energies in the assignment of surface reaction products: ethyne and ethene on Ni{110}. J. Molec. Catal. A: Chem. 141, 21–29.

Brzić, D., Petkovska, M., 2012. Some practical aspects of nonlinear frequency response method for investigation of adsorption equilibrium and kinetics. Chem. Eng. Sci. 82, 62–72.

Garayhi, A.R., Keil, F.J., 2001. Modeling of microkinetics in heterogeneous catalysis by means of frequency response techniques. Chem. Eng. J. 82, 329–346.

Hertz, R., 2015. Scaling parameters for dynamic diffusion-reaction over porous catalysts. Ind. Eng. Chem. Res. 54, 4095–4102.

Hoebink, J., Nievergeld, A., Marin, G., 1999. CO oxidation in a fixed bed reactor with high frequency cycling of the feed. Chem. Eng. Sci. 54, 4459–4468.

Iijima, Shun-ichiro, 1940. The adsorption of ethylene on reduced nickel. Rev. Phys. Chem. Jpn. 14 (2), 68–78.

Kalz, K., Kraehnert, R., Dvoyashkin, M., Dittmeyer, R., Gläser, R., Krewer, U., Reuter, K., Grunwaldt, J.-D., 2017. Future challenges in heterogeneous catalysis: understanding catalysts under dynamic reaction conditions. ChemCatChem 9, 17–29.

Kočí, P., Kubíček, M., Marek, M., 2004. Periodic forcing of three-way catalyst with diffusion in the washcoat. Catal. Today 98, 345–355.

Li, Y.-E., Willcox, D., Gonzalez, R.D., 1989. Determination of rate constants by the frequency response method: CO on Pt/SiO_2. AIChE J. 35 (3), 423–428.

Lie, A., Hoebink, J., Marin, G., 1993. The effects of oscillatory feeding of CO and O_2 on the performance of a monolithic catalytic converter of automobile exhaust gas: a modelling study. Chem. Eng. J. 53, 47–54.

Marcelin, G., Lester, J., Mitchell, S., 1986. Frequency response study of the effect of alkali promotion on Rh/TiO_2 catalysts: evidence for kinetically distinct H_2-sorbing sites. J. Catal. 102, 240–248.

Marković, A., Seidel-Morgenstern, A., Petkovska, M., 2008. Evaluation of the potential of periodically operated reactors based on the second order frequency response function. Chem. Eng. Res. Design 86, 682–691.

Meyer, D., Friedland, J., Kohn, T., Güttel, R., 2017. Transfer functions for periodic reactor operation: fundamental methodology for simple reaction networks. Chem. Eng. Technol. 40 (11), 2096–2103.

Nievergeld, A., 1998. Automotive Exhaust Gas Conversion: Reaction Kinetics, Reactor Modelling and Control Dissertation. Technische Universiteit Eindhoven.

Park, I., Petkovska, M., Do, D., 1998. Frequency response of an adsorber with modulation of the inlet molar flow-rate—II. A continuous flow adsorber. Chem. Eng. Sci. 53, 833–843.

Petkovska, M., Nikolić, D., Seidel-Morgenstern, A., 2018. Nonlinear frequency response method for evaluating forced periodic operations of chemical reactors. Isr. J. Chem. 58, 663–681.

Poling, B., Prausnitz, J.M., O'Connell, J.P., 1988. The Properties of GASES AND LIQUIDS. McGraw-Hill.

Radhakrishnan, K., Hindmarsh, A., 1993. Description and Use of LSODE, the Livermore Solver for Ordinary Differential Equations. NASA Reference Publication 1327 Lawrence Livermore National Laboratory Report UCRL-ID-113855.

Reyes, S.C., Sinfelt, J.H., DeMartin, G.J., 2005. Frequency response study of the dynamics of the platinum catalyzed interconversion of methylcyclohexane, toluene, and hydrogen near equilibrium. J. Phys. Chem. B 109, 2421–2431.

Silveston, P., Hudgins, R.R., Renken, A., 1995. Periodic operation of catalytic reactors – introduction and overview. Catal. Today 25, 91–112.

Spivey, J., Agarwal, S., Reyes, S., Iglesia, E., 1994. Frequency response techniques for the characterization of porous catalytic solids. Catal., Spec. Period. Rep. 11, 51–92.

Thullie, J., Renken, A., 1993. Model Discrimination for Reactions with a Stop-effect. Chem. Eng. Sci. 48 (392), 1–3925.

van Neer, F., Kodde, A., Den Uil, H., Bliek, A., 1996. Understanding of resonance phenomena on a catalyst under forced concentration and temperature oscillations. Can. J. Chem. Eng. 74 (5), 664–673.

Watanabe, N., Onogi, K., Matsubara, M., 1981. Periodic control of continuous stirred tank reactors—I: the pi criterion and its applications to isothermal cases. Chem. Eng. Sci. 36 (5), 809–818.

Yasuda, Y., Suzuki, Y., Fukada, H., 1991. Kinetic details of a gas/porous adsorbent system by the frequency response method. J. Phys. Chem. 95, 2486–2492.

Yoshida, F., Ramaswami, D., Hougen, O., 1962. Temperatures and partial pressures at the surfaces of catalyst particles. AIChE J. 8 (5).